



Fabrication of tunable pore size of nickel membranes by electrodeposition on colloidal monolayer template

Jian-Hong Lee^a, Yi-Wen Chung^a, Min-Hsiung Hon^b, Ing-Chi Leu^{c,*}

^a Laser Application Technology Center, Industrial Technology Research Institute, Tainan County, 734, Taiwan, ROC

^b Department of Materials Science and Engineering, National Cheng Kung University, Tainan, 701, Taiwan, ROC

^c Department of Materials Science, National University of Tainan, Tainan, 700, Taiwan, ROC

ARTICLE INFO

Article history:

Received 21 July 2010

Received in revised form 8 March 2011

Accepted 8 March 2011

Available online 4 April 2011

Keywords:

Nanosphere lithography
Electrochemical deposition
2D ordered array

ABSTRACT

Large-area nickel patterned membranes with tunable pore size are prepared by the combination of self-assembly nanosphere lithography and electrodeposition. The morphology of the nickel membranes exhibits a honeycomb or egg-shell-roofed structure depending on the deposition time and the electrostatic-induced absorption effect. With an increase of electrodeposition time, the movement of polystyrene spheres caused by metal-filling gradually changes the contact evolution between the spheres and the substrate from facet contact to quasi-point contact, until complete lift from the substrate. Hence, the pore size can be controlled by varying the deposition time; i.e., by controlling the contact area between the polystyrene spheres and the substrate. Such membranes can be useful as templates for nanofabrication. The site and density control of one-dimensional nanostructures, depending on the distance and the size of the pore, is a critical issue in many potential applications, such as optical antennas, biosensors and bioprobes, and field emission devices.

© 2011 Elsevier B.V. All rights reserved.

1. Introduction

The fabrication and structural characterization of periodic structures in the submicron scale are topics of great interest in the field of nanotechnology. Surface-patterned micro- and nanostructures have many applications in several scientific and technological fields, such as electronic and optical devices [1], photonic materials [2], and templates for fabricating biological and chemical sensors [3]. Various lithography techniques, such as those based on scanning probe, electron beam, focused ion beam, or X-ray, have been routinely used to fabricate two-dimensional (2D) metallic periodic arrays [4–6]. However, the application of these conventional techniques is limited by the high cost and low processing speed. Thus, nanosphere lithography (NSL) has recently attracted attention for the fabrication of ordered nanostructures over large areas [7,8]. In this process, the latex particles self-organize into an ordered pattern, and then the desired materials are deposited onto the ordered colloidal spheres to obtain a 2D arrays [9,10].

Morphology-controlled ordered nickel porous arrays are of importance in fundamental research due to their morphology-dependent electric, magnetic properties and also with regard to

practical applications [11–13]. Recently, Duan [14,15] reported the electrochemical synthesis of 2D ordered porous nickel arrays based on a polystyrene sphere colloidal monolayer. The morphologies can be controlled from a bowl-like structure to a hollow sphere-like structure by changing deposition time under a constant current.

The present study presents a simple approach that combines the self-assembled monolayer mask technique with electrodeposition for preparing ordered patterned membranes after the removal of polystyrene spheres. The pore size of the patterned membrane can be adjusted by changing the deposition time of the electrodeposition process. Furthermore, the pore size whether the topmost layer of the structure is open or closed. In addition, the detailed changes of the morphology at each stage under constant voltage (–1 V) are also discussed.

2. Experimental procedures

Polystyrene spheres were prepared via dispersion polymerization. The substrate was processed by a surface treatment to increase the wettability and smoothness of the substrate. Si substrate was pretreated in two steps to render a hydrophilic surface; the first was with piranha etching by 3:1 H₂SO₄:30% H₂O₂ at 80 °C for 1 h, and then base treatment by 5:1:1 H₂O:30% H₂O₂:NH₄OH with sonication for 1 h. A monolayer of latex spheres was created by the spin coating of 1.2-μm-diameter polystyrene spheres onto a Si substrate using a custom-built spin coater. The spin coating was performed at a speed of 3000 rpm. The latex solution from the manufacturer was diluted in a solution of surfactant Triton X-100/methanol (1:1000 by volume) in a ratio of 1:4–1:5 (by volume) before the spin coating process. The quality and thickness of colloidal crystals are greatly affected by the spin speed, concentration of the colloidal suspension, rheology of the suspension, and wet-

* Corresponding author at: National University of Tainan, Department of Materials Science, 33, Sec. 2, Shu-Lin St., Tainan City 700, Taiwan, ROC. Tel.: +886 6 2380208; fax: +886 6 2380208.

E-mail address: icleu@mail.mse.ncku.edu.tw (I.-C. Leu).

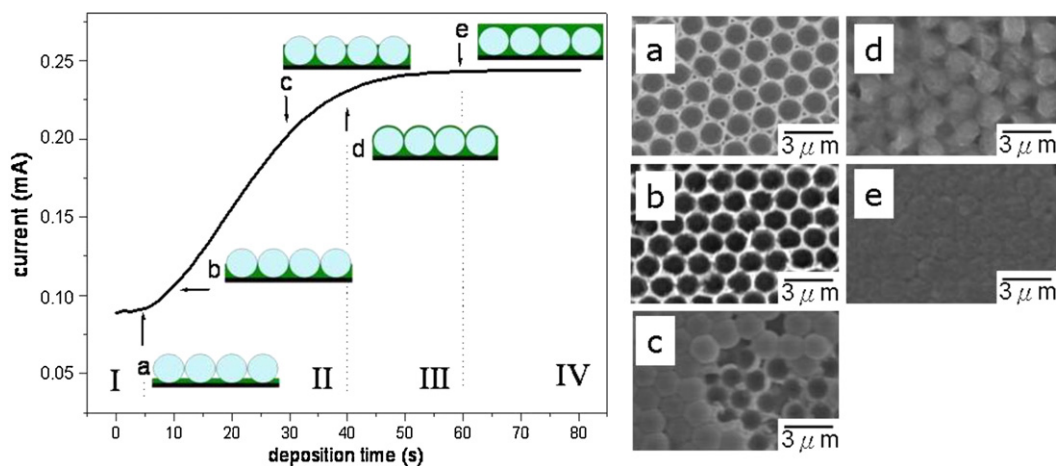


Fig. 1. The relationship between electrodeposition current and time shows the stages of the formation of nickel inside the polystyrene template at each point, as indicated by the arrows.

tability of substrate. The aqueous solution used for nickel electrodeposition was composed of $\text{NiSO}_4 \cdot 6\text{H}_2\text{O}$, $\text{NiCl}_2 \cdot 6\text{H}_2\text{O}$, and H_3BO_3 . After the deposition process, the samples were dried in air, followed by subsequent removal of the polystyrene spheres by dissolution in dichloromethane solvent for 10 mins. The surface roughness of the nickel deposit was analyzed with the aid of an atomic force microscope (AFM, Digital Instrument Nanoscope). After the polystyrene spheres were removed using dichloromethane, a nickel membrane with 2D ordered and patterned pores remains. The products obtained were characterized by field-emission scanning electron microscopy (Hitachi S-3000 N).

3. Results and discussion

Fig. 1 shows the current changes during the electrodeposition process along with the resulting film morphologies. By adjustment of the microsphere size and the applied current, the proposed method allows for precise control over the structure formation and film thickness of the obtained nickel films. Three stages can be clearly observed for the entire process of nickel filling the interstitial spaces of a colloidal array [16]. In the first stage, from 0 to 5 s, nickel ions are attracted to the electrode and reduced to nickel metal; they nucleate and form a nickel film on the substrate. In the second stage from 5 to 40 s, the nickel metal fills the interstitial spaces of the polystyrene template from bottom to top. In this stage, the current increases very sharply at point c in the curve, which is ascribed to a rapid increase of the nickel metal area once the growth front of the deposited material reaches the template/bulk solution interface [17]. This is confirmed in our experiments where the electrodeposition process was stopped at various stages, as indicated by the arrows and corresponding SEM images of the 2D nickel films obtained at each stage (also shown in Fig. 1). If the electrodeposition process is stopped at a very early stage ((b), before 40 s), a bowl-like nickel array is obtained. If the electrodeposition process is stopped at a later stage ((b), after 40 s), an egg-shell-roofed nickel structure is obtained. Fig. 1(c) shows that some of the pores at the top layer begin to close; if the process is continued, then all the pores at the topmost layer closed. In the third stage, from 40 to 60 s, the polystyrene template is covered completely by the nickel metal. Beyond this point, at the fourth stage, the occurrence of nickel electroplating on the planar coating can be found above the surface of the polystyrene template.

In order to further explain the formation of egg-shell-roofed nickel films during the electrodeposition process, an investigation on the effect of the surface charge of polystyrene was conducted. After 60 s of deposition, the egg-shell-roofed nickel films are obtained, as shown in Fig. 2(a). Fig. 2(b) and (c) shows the zeta-potential of polystyrene colloidal particles in water and polystyrene colloidal particles dispersed in the aqueous nickel electroplating

solution, respectively. The average values of zeta-potential for the two cases, in water and electroplating solution, are -19.5 and -10.3 mV, respectively. The results indicate that positively charged nickel ions adsorb onto the surface of negatively charged colloidal particles, when they migrate near the colloidal particles [14], due to the electrostatic-induced adsorption effect in the electrodeposition solution. When the electrodeposition process starts, the nickel ions, which are away from the colloidal crystal template, will migrate toward the working electrode as they are attracted by the applied potential (-1 V), resulting in an increase of the nickel ion concentration [18]. Hence, in this situation the colloidal particles constructing the template adsorb more nickel ions than they do in the case without the application of potential. The process of nickel ions reducing to metal and filling the interstitial spaces at the template bottom takes place simultaneously with the adsorption of nickel ions onto the colloidal surface at the template top. Furthermore, the nickel ions continuously adsorb onto the colloidal surfaces at the template top, until the height of the nickel filling the interstitial spaces reaches the template surface. Nickel metal grows preferentially on the colloidal surface compared to sites among the colloids [19], and thus a nickel egg-shell-roofed film is obtained after the removal of the polystyrene colloidal template by accurately controlling the electrodeposition mechanism.

The polystyrene colloidal template with quasi-point contact was used to fabricate ordered patterns. Fig. 3 shows ordered nickel structure formation on a Si substrate produced by electrodeposition for 10–30 s and schematic illustrations of the area of the nickel template (region outside the white circle) and original polystyrene-covered area (white circle). The pore size of the nickel template and original polystyrene-covered area are shown in the inset of Fig. 3(c), represented as black and white dotted circles, respectively. The original polystyrene covered area at the bottom is found to decrease with the increase of the electrodeposition time. The electrodeposition was carried out at a constant potential for various deposition times. Fig. 4 shows AFM images of the surface morphology of the electrodeposited nickel films at -1 V for 20 s. The surface appears to have a uniform distribution of granular-shaped grains. Fig. 5 shows schematic cross-section illustrations of the mechanism for nickel filling into the 2D colloidal crystal template and the lift of polystyrene during the electrodeposition process. Fig. 5(a) shows that the polystyrene microspheres take on a hexagonal closely packed lattice structure. Once the 2D polystyrene sphere array forms on the substrate, the height of the walls of the bowls is precisely controlled by the time of the electrodeposition process. When the electrodeposition begins, nickel crystal nuclei form on the substrate (electrode) and wedge-shaped regions between the

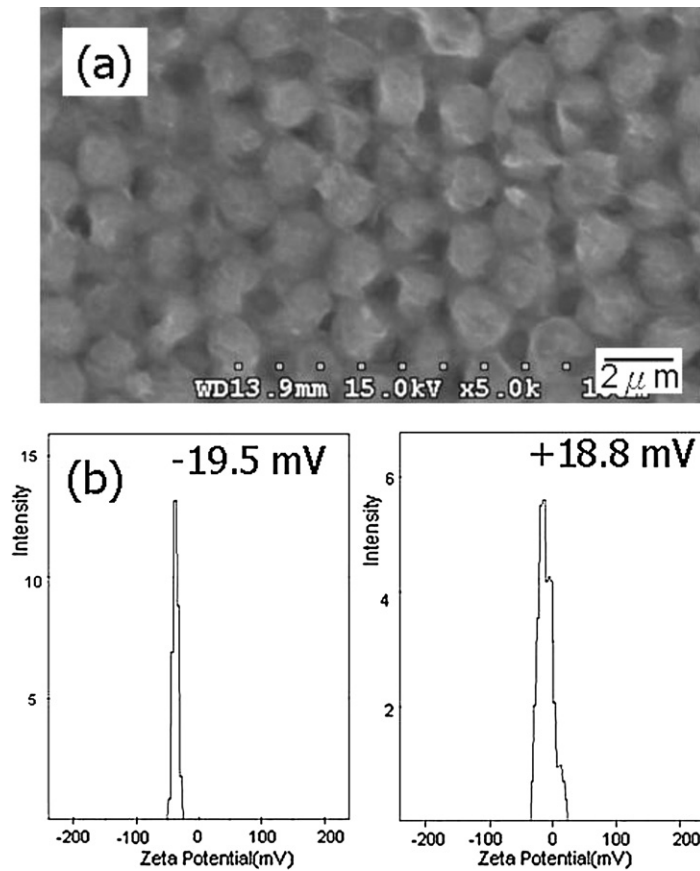


Fig. 2. (a) SEM images of egg-shell-roofed nickel film and the measured zeta-potential for polystyrene colloidal particles in (b) water and (c) the nickel electrolytic deposition solution.

polystyrene colloidal spheres due to the lower energy barrier of nucleation in this area, as shown in Fig. 5(a). Nickel ions are reduced to metal and fill the interstitial spaces at the template bottom. If the electrodeposition process is continued, the nickel-filling height

reaches the contact site between the polystyrene spheres. Fig. 5 (b) shows an enlarged image of the interface of the polystyrene and electrodeposited nickel films. Voids exist at the interface of the polystyrene and electrodeposited nickel films due to the surface

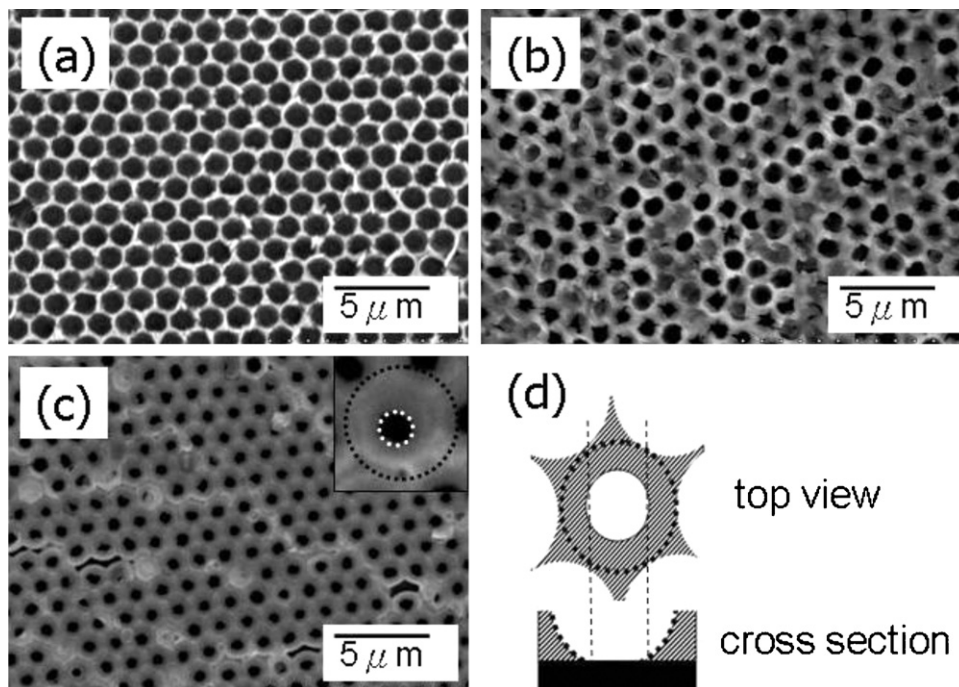


Fig. 3. SEM images of the ordered structure formation on a Si substrate by electrodeposition for deposition times of (a) 10, (b) 20, and (c) 30 s. (d) Schematic illustrations of the area of the nickel template and original polystyrene-covered area.

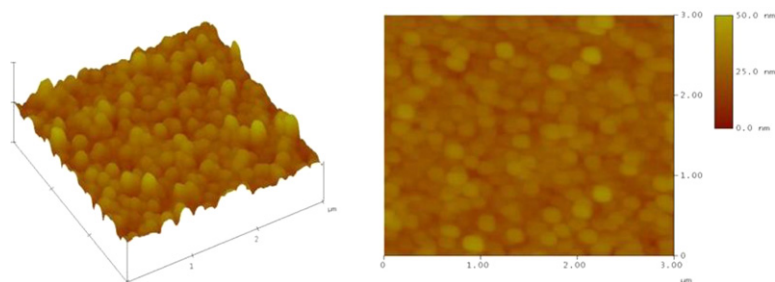


Fig. 4. AFM images of the electrodeposited nickel thin films.

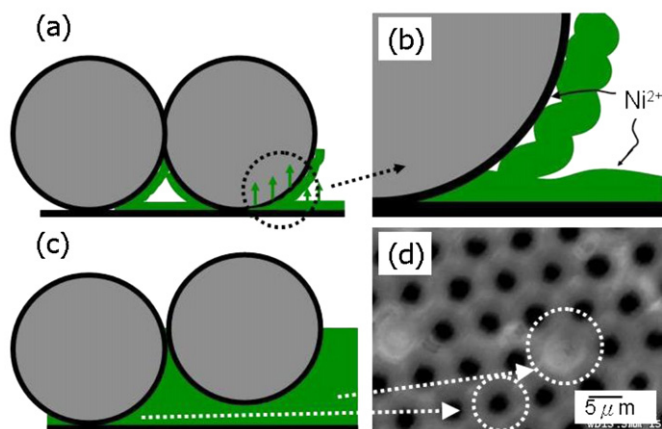


Fig. 5. Schematic illustrations of the mechanism of nickel filling a 2D colloidal crystal template and the movement of polystyrene during the electrodeposition process.

roughness caused by the granular-shaped grains of the nickel film (see Fig. 4). In the electrodeposition of metals, the nickel ions are transported from the solution to the surface of the electrode by diffusion. Voids at the interface of the polystyrene and electrodeposited nickel films can be used as the channels for the nickel ion transportation during the electrodeposition process. As the deposition process continues, nickel metal will fill in the voids and slowly move the polystyrene spheres. The initial contact for the 2D polystyrene sphere array formed on the substrate is facet contact. With continued deposition, the contact area gradually reduces to quasi-point contact, and the polystyrene spheres move away from the substrate. As a result, the pores are filled, as shown in the dotted circles in Fig. 5(c) and (d). During the electrodeposition process, voids exist at the interface of the polystyrene and electrodeposited nickel films due to the surface roughness caused by the granular-shaped grains of nickel film. The nickel ions reduce to metal and fill the voids simultaneously. The movement of polystyrene spheres caused by the metal filling gradually changes the contact between the spheres and the substrate from facet contact to quasi-point contact, until complete lift from the substrate. Therefore, the pore size can be controlled by controlling the deposition time; i.e., by controlling the contact area between the polystyrene spheres and the substrate.

4. Conclusions

An electrodeposition approach based on a colloidal template was presented and a series of large-area and ordered pore membranes was synthesized. This structure is useful for selecting spheres smaller than the inner diameter of the bowls [20]; such bowls may also be useful for novel biomedical applications and nanofluidic devices method may allow the creation of patterned

1D nanostructures, such as ZnO [21], CNT, and other materials for applications as sensor arrays [22], piezoelectric antennas arrays [23], and optoelectronic devices [24]. These patterned macroporous membranes with well-defined pore sizes have promising applications in the areas of filtration, chemical delivery, and chemical sensing, as well as templates for fabricating other ordered nanostructures [25,26]. These patterned macroporous allow a more controllable process conditions for various applications, such as interface reaction, accurate drug carrying capacity, and adjustable sensing area.

Acknowledgement

The financial supports through contract numbers NSC96-2221-E-006-119-MY3 and NSC96-2628-E-239-002-MY3 by the National Science Council, Taiwan ROC are greatly appreciated.

References

- [1] J. Heiko, G.M. Whitesides, *Science* 291 (2001) 1763–1766.
- [2] P. Jiang, J. Cizeron, J.F. Bertone, V.L. Colvin, *J. Am. Chem. Soc.* 121 (1999) 7957–7958.
- [3] H. Kim, R.E. Cohen, P.T. Hammond, D.J. Irvine, *Adv. Funct. Mater.* 16 (2006) 1313–1317.
- [4] T. Yasuda, S. Yamasaki, S. Gwo, *Appl. Phys. Lett.* 77 (2000) 3917–3919.
- [5] J.I. Martin, J. Nogués, K. Liu, J.L. Vicent, I.K. Schuller, *J. Magn. Magn. Mater.* 256 (2003) 449–501.
- [6] S. Anders, S. Sun, C.B. Murray, C.T. Rettner, M.E. Best, T. Thomson, M. Albrecht, J.U. Thiele, E.E. Fullerton, B.D. Terris, *Microelectron. Eng.* 61 (2002) 569–575.
- [7] A.K. Sirvastava, S. Madhavi, T.J. White, R.V. Ramanujan, *J. Mater. Chem.* 15 (2005) 4424–4428.
- [8] F. Burmeister, C. Schöfle, T. Matthes, M. Böhmsch, J. Boneberg, P. Leiderer, *Langmuir* 13 (1997) 2983–2987.
- [9] F.Q. Zhu, D.L. Fan, X.C. Zhu, J.G. Zhu, R.C. Cammarata, C.L. Chien, *Adv. Mater.* 16 (2004) 2155–2159.
- [10] L.P. Li, Y.F. Lu, D.W. Doerr, D.R. Alexander, J. Shi, J.C. Li, *Nanotechnology* 15 (2004) 333–336.
- [11] Z. Huang, D.L. Carnahan, J. Rybczynski, M. Giersig, M. Sennett, D. Wang, J. Wen, K. Kempa, Z. Ren, *Appl. Phys. Lett.* 82 (2003) 460–465.
- [12] L. Maya, T. Thundat, J.R. Thompson, R.J. Stevenson, *Appl. Phys. Lett.* 67 (1995) 3034–3036.
- [13] Y.L. Tai, H. Teng, *Chem. Mater.* 16 (2004) 338–342.
- [14] G. Duan, W. Cai, Y. Luo, Z. Li, Y. Lei, *J. Phys. Chem. B* 110 (2006) 15729–15733.
- [15] G. Duan, W. Cai, Y. Li, Z. Li, Bi. Cao, Y. Luo, *J. Phys. Chem. B* 110 (2006) 7184–7188.
- [16] T. Sumida, Y. Wada, T. Kitamura, S. Yangagida, *Chem. Commun.* 17 (2000) 1613–1614.
- [17] S. Tian, J. Wang, U. Jonas, W. Knoll, *Chem. Mater.* 17 (2005) 5726–5730.
- [18] Y.W. Chung, I.C. Leu, J.H. Lee, J.H. Yen, M.H. Hon, *Electrochim. Acta* 53 (2007) 1703–1707.
- [19] M.L. Povinelli, S.G. Johnson, J.D. Joannopoulos, *Appl. Phys. Lett.* 82 (2003) 1069–1071.
- [20] X.D. Wang, E. Graugnard, J.S. King, Z.L. Wang, C.J. Summers, *Nano Lett.* 4 (2004) 2223–2226.
- [21] J.H. Lee, Y.W. Chung, M.H. Hon, I.C. Leu, *Appl. Phys. A* 97 (2009) 403–408.
- [22] M.S. Arnold, Ph. Avouris, Z.W. Pan, Z.L. Wang, *J. Phys. Chem. B* 17 (2003) 659–663.
- [23] X.Y. Kong, Z.L. Wang, *Nano Lett.* 3 (2003) 1625–1631.
- [24] P. Avouris, Z. Chen, V. Perebeinos, *Nat. Nanotechnol.* 2 (2007) 605–615.
- [25] F. Yan, W.A. Goedel, *Nano Lett.* 4 (2004) 1193–1196.
- [26] H.X. Xu, W.Y. Rao, J. Meng, Y. Shen, C.J. Jin, X.H. Wang, *Nanotechnology* 20 (2009) 465608–465613.